



# What is the eco-toxicological level and effects of graphene oxide-boramic acid (GO-ED-BA NP)?: In vivo study on Zebrafish embryo/larvae

Mine Köktürk<sup>a,b,\*</sup>, Serkan Yildirim<sup>c</sup>, Aybek Yiğit<sup>b,d</sup>, Günes Ozhan<sup>e,f</sup>, İsmail Bolat<sup>c</sup>, Mehmet Hakkı Alma<sup>g</sup>, Nurettin Menges<sup>d,\*\*</sup>, Gonca Alak<sup>h,\*\*</sup>, Muhammed Atamanalp<sup>i,\*\*</sup>

<sup>a</sup> Department of Organic Agriculture Management, Faculty of Applied Sciences, Iğdir University, TR-76000 Iğdir, Turkey

<sup>b</sup> Research Laboratory Application and Research Center (ALUM), Iğdir University, TR-76000 Iğdir, Turkey

<sup>c</sup> Department of Pathology, Veterinary Faculty, Ataturk University, TR-25030 Erzurum, Turkey

<sup>d</sup> Pharmaceutical Chemistry Section, Pharmacy Faculty, Van Yüzüncü Yıl University, TR-65080 Van, Turkey

<sup>e</sup> İzmir Biomedicine and Genome Center (IBG), Dokuz Eylül University Health Campus, TR-35340 İzmir, Turkey

<sup>f</sup> İzmir International Biomedicine and Genome Institute (IBG-Izmir), Dokuz Eylül University, TR-35340 İzmir, Turkey

<sup>g</sup> Department of the Biosystems Engineering, Faculty of Agriculture, Iğdir University, TR-76000 Iğdir, Turkey

<sup>h</sup> Department of Aquaculture, Faculty of Fisheries, Ataturk University, TR-25030 Erzurum, Turkey

<sup>i</sup> Department of Seafood Processing Technology, Faculty of Fisheries, Ataturk University, TR-25030 Erzurum, Turkey

## ARTICLE INFO

Editor: Pei Xu

### Keywords:

Graphene oxide  
Boric acid  
Zebra fish  
DNA damage  
cytokine

## ABSTRACT

Graphene oxide (GO) and their natural/synthetic composites are encouraging tools for humanity. There is a need to address critical challenges and potential risk possibilities in GO-based architectures, which have a wide range of uses. In this study, ecotoxicological levels as well as GO-based nanoparticle synthesis, characterization, interaction mechanism and toxicity detection levels for potential biomedical applications were determined on zebrafish (*Danio rerio*). The effects of GO-ED-BA NP (graphene oxide-boramic acid nano particles) which was characterized by FT-IR, SEM, TEM, and BET on survival rate, morphological abnormalities (yolk sac edema, lordosis/kyphosis, pericardial edema, and tail malformation), hatching rate as well as neuronal degeneration /necrosis, 8 OHdG and TNF- $\alpha$  expression were observed in *D. rerio* embryos and larvae. In the obtained findings, it was determined that the toxicity profile of GO-ED-BA NP appeared similar, in high-dose application with single GO use, causing a cytotoxic, pro-inflammatory response and triggering oxidative stress. However, increased malformation rates and mortality at the highest concentration were due to nanoparticle sizes and GO. The presence of boramic acid unit on graphene nanostructure changed the GO's toxicity profile and positively directed the proinflammatory and oxidative stress response. Synthesizing of graphene oxide-boramic acid and its toxicity panels compared to graphene oxide are reported for the first time in this study.

## 1. Introduction

Especially in recent years, advances in nanotechnology have had significant effects with the introduction of nanoparticles (NP) to the pharmaceutical industry. Increasing drug solubility, modulating drug release properties, targeting drug molecules to desired regions and delivering more than one drug at the same time are among these important effects. Due to these unique advantages, a number of NP-based drug delivery systems had been approved for clinical use that can improve the pharmacokinetic profile and therapeutic index of drug

loads [14,17].

Especially recently, antimicrobial nanoparticle formulations have been increasingly researched and innovative approaches are emerging that focus on alternative products. Among these innovative products, graphene is a highly attractive compound due to its properties (good mechanical strength, high surface area, elasticity, hardness, excellent biocompatibility, outstanding a variety of properties, superior electrical and thermal conductivity, and ease of functionalization) [29]. Despite its short history, graphene had attracted great interest in the scientific and industrial communities all over the world, and it has been

\* Corresponding author at: Department of Organic Agriculture Management, Faculty of Applied Sciences, Iğdir University, TR-76000 Iğdir, Turkey.

\*\* Correspondence to: Faculty of Fisheries, Ataturk University, TR-25030 Erzurum, Turkey.

E-mail addresses: [mine.kokturk@igdir.edu.tr](mailto:m.kokturk@igdir.edu.tr) (M. Köktürk), [nurettinmenges@yyu.edu.tr](mailto:nurettinmenges@yyu.edu.tr) (N. Menges), [galak@atauni.edu.tr](mailto:galak@atauni.edu.tr) (G. Alak), [mataman@atauni.edu.tr](mailto:mataman@atauni.edu.tr) (M. Atamanalp).

<https://doi.org/10.1016/j.jece.2022.108443>

Received 9 May 2022; Received in revised form 28 June 2022; Accepted 12 August 2022

Available online 17 August 2022

2213-3437/© 2022 Elsevier Ltd. All rights reserved.

recognized as a promising nanomaterial for many applications. The number of publications on graphene hybrids and their catalytic applications (according to ISI Web of Knowledge) had increased significantly after 2004 and is around 1000 (until August 23, 2020). Graphene oxide (GO) from graphene with different forms [pure/pure graphene,  $-\text{CO}-$ ,  $-\text{COOH}$  or  $-\text{COH}$  containing graphene oxide (GO), reduced GO (rGO) and animated graphene oxide (AGO)], variable for effective chemical interactions are excellent support materials due to their functionality and receive special attention [1]. As a result of these versatile applications, the release of GO into the ecosystem is inevitable, and its risks associated with the critical period of embryogenesis are largely unknown [11].

To avoid NP-induced problems in biological systems, various research groups had sought help from different chemical and biological agents to modify surfaces and stop loss. Surface modification by natural or synthetic polymers creates more stable, hydrophilic nanostructures and provides a relatively large number of variable functional groups on the surface that aid in the proper attachment of interactomes to nanostructures [6]. In recent years, boric acid (BA) compounds with three hydroxyl groups and weak acidity, had been used for different purposes (increasing heat resistance, mechanical strength and gas barrier) in various composites [40].

With the rapid development and application of these materials, understanding the adverse effects of nanomaterials is critical for their optimization and management. In line with the explanations above, in this study, ethylenediamine (ED) and nontoxic BA modified GO-ED-BA NPs as precursors were prepared to formulate the GO origin nanoparticle preparation.

This study aimed to investigate the toxic effect and molecular mechanism of GO-ED-BA NPs in zebrafish embryo/larvae. Another aim of this study was to examine the toxic effects of appropriate modifications on the surface of graphene oxide, which is a good nanomaterial, and to contribute to the development of new nanomaterials that will have a very low or acceptable level of toxic value for different applications in the future. Menges and his research group published carbon nanotube-boramic acid structure for electrochemical determination of dopamine in a real sample [39]. Mentioned study was the first example of carbon nanotube-boramic acid. In our current study, we changed the nanostructure to graphene oxide, which gave a larger surface. Modifying the oxide units on the nanostructure with ethylenediamine and boric acid revealed graphene oxide-boramic acid for the first time, and new nanostructure and its characterization might be important source for further modifications. Moreover, the study shows that the boramic acid functional group can contribute to different research areas as *in vitro* and *in vivo* applications. Based on this information, we desire to investigate and see how this modification changed the toxic effect *in vivo* in detail. It is worthy to say that structure-activity relationship (SAR) with three different nanostructures might give a perspective for further studies. With this study, it is predicted that the graphene oxide-boramic acid structure, which has been introduced to the literature for the first time, can be a source of inspiration for many different applications and new modifications thanks to boron chemistry [9,41] and graphene oxide-nano composite [27]. In addition, this study was aimed to investigate the toxic effect with molecular mechanism of GO-ED-BA NPs in zebrafish embryo/larvae.

## 2. Materials and methods

### 2.1. Reagents for chemistry

Thionyl chloride ( $\text{SOCl}_2$ ), dimethylformamide (DMF), anhydrous tetrahydrofuran (THF), ethylenediamine, boric acid, graphite, sodium nitrate, sulfuric acid ( $\text{H}_2\text{SO}_4$ ), potassium permanganate ( $\text{KMnO}_4$ ), hydrogen peroxide ( $\text{H}_2\text{O}_2$ ), were purchased from Sigma-Aldrich.

### 2.2. Synthesis of GO-ED-BA nanoparticles

#### a. Formation of GO-Cl

Graphene oxide (GO) was prepared according to the Hummers method [10]. Next, GO-COOH (300 mg) was placed in a 25 mL glass vial, followed by  $\text{SOCl}_2$  (10 mL) and dry DMF (1 mL) were added sequentially. The reaction medium was heated at  $70^\circ\text{C}$  for 24 h. After the heating was completed, filtration was performed on a gooch crucible (No: 4) to separate the solid from the solution. During filtration through a Gooch crucible (No: 4), the solid was washed first with dry diethyl ether, dry THF and finally dry DMF. The solid obtained after washing was dried in a vacuum oven at  $50^\circ\text{C}$  for 24 h. Then, FT-IR, SEM, TEM, and BET were utilized for surface characterizations (Fig. 1).

#### b. Formation of GO-ED

GO-Cl (100 mg) was taken into a glass flask (25 mL) and 4 mL of ethylenediamine was added and the reaction medium was heated at  $110^\circ\text{C}$  for 24 h. After heating, filtration was performed in a gooch crucible (No: 4) and the resulting solid was washed with dry THF. In the next step, it was dried in a vacuum oven at  $50^\circ\text{C}$  for 24 h for surface information. Then, surface characterizations were performed (Fig. 2).

#### c. Formation of GO-ED-BA

GO- $\text{NH}_2$  (100 mg) and 5 mL DMF were placed in a glass balloon (25 mL) and mixed for a while. Then, boric acid (300 mg) was added thereto and the reaction medium was heated at  $120^\circ\text{C}$  for 24 h. After heating, filtration was done on the gooch crucible (No: 4) to separate the solid from the solution. During filtration, the solid was washed first with purified water, THF, and then finally with ethyl alcohol. The solid obtained after washing was dried in a vacuum oven at  $50^\circ\text{C}$  for 24 h. Then, surface analysis was performed with appropriate equipment (Fig. 3) [39].

#### d. Characterization of modified GO

The samples' structure characterization was carried out using a Zeiss Sigma 300 scanning electron microscope (SEM) with inlens detector at 10 kV accelerating voltage and Transmission Electronic Microscopy (TEM) with Hitachi High-Tech HT7700 (120.0 kV). Analyzes  $\text{N}_2$  adsorption-desorption measurements (BET) were performed with Micromeritics 3 Flex brand device. Analyzes were performed at Van Yüzüncü Yıl University Science and Application Center, Iğdır University Research Laboratory Application and Research Center (ALUM), and Atatürk University (DAYTAM) Research Center.

### 2.3. Zebrafish

The source of zebrafish was Izmir Biomedicine and Genome Center (Turkey). They were kept (at  $28^\circ\text{C}$  with a 14 h light/10-h dark cycle) and bred according to standard procedures [35]. Fish were fed at 9 a. m–3 p.m, the morning feeding was with flake food (TetraMin Tropical Flakes 48% protein, 8% fat, and 2% fiber), and the second one was done with Artemia. Younger than 5-day-old zebrafish larvae were used in the study. Thus, the study does not require any license (Directive 86/609/EEC and EU Directive, 2010/63/EU). The selected fish were transferred to breeding tanks around 5–6 pm at a 1:1 female: male ratio and kept overnight. The next morning, zebrafish were stimulated by light to mate and lay eggs. Embryos were collected and transferred to petri dishes and kept at  $28^\circ\text{C}$  until analyses [19].

### 2.4. GO-ED-BA NP exposure to zebrafish embryos and nanotoxicity testing

The exposure concentrations for embryos were determined with reference to de Medeiros et al., [25]. Stock solutions of GO, GO-ED and GO-ED-BA were prepared with distilled water (containing 0.01% DMSO) and sonicated (Minichiller Diagenode, 50/60 kHz, Huber, Germany) for

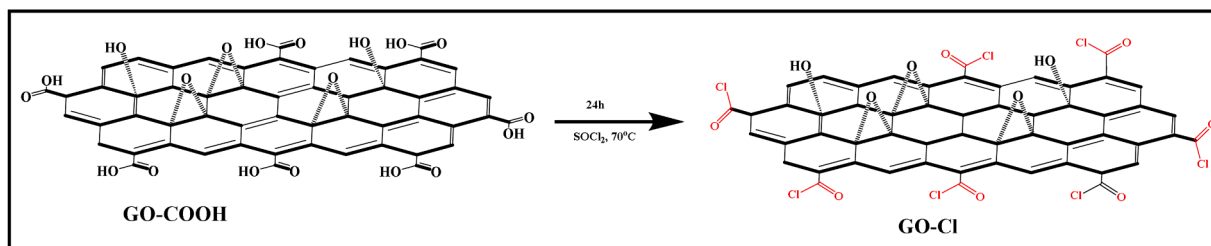


Fig. 1. Synthesis of GO-Cl.

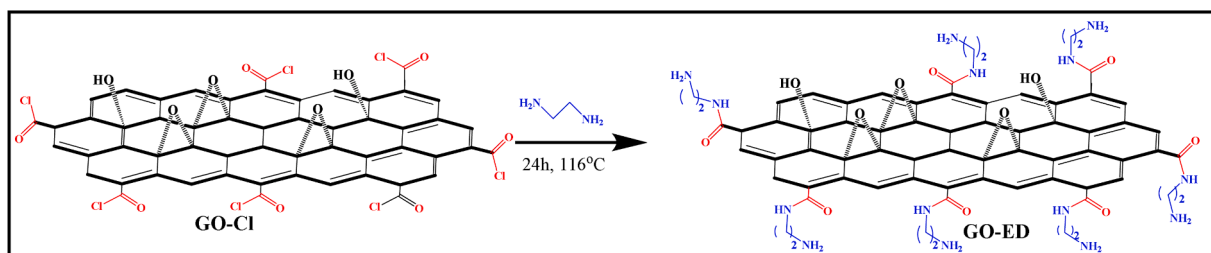


Fig. 2. Ethylene diamine modification on the GO surface.

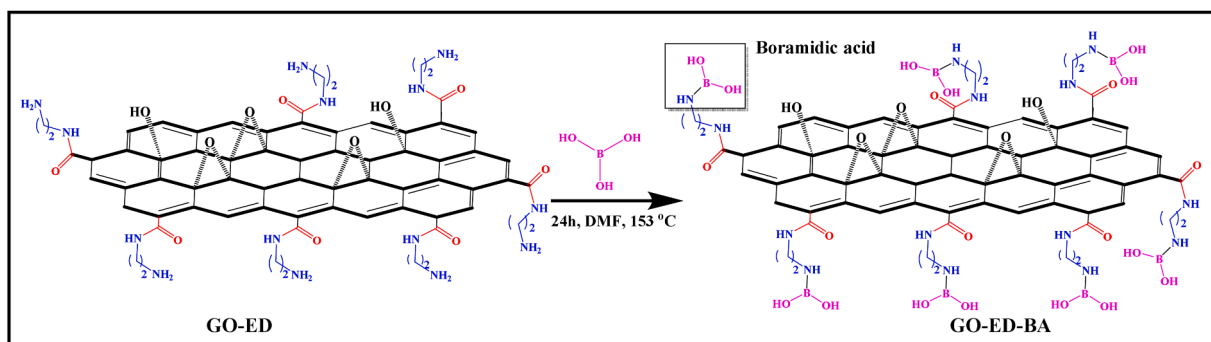


Fig. 3. Modification of the GO-ED surface with boric acid.

30 min

Different concentrations (0.1, 0.5 and 1 mg/mL) were prepared from the prepared stock solutions for each product and applied to the experimental groups (Table 1) by renewing the experimental medium every day. 20 embryos were used for each group and the experiment was repeated three times. The trial was started at the 4th hour after fertilization, continued for 96 h, and all applications were continued under the same conditions. The survival rate, larval hatching rate and morphological changes were followed in the 24–96 hpf range. Changes

**Table 1**

The trial groups and contents.

Treatment group	Treatment content
Control	E3: 0.17 mM KCl, 0.33 mM MgSO4, 5 mM NaCl ve 0.33 mM CaCl2
DMSO	% 0.01 DMSO with E3
0.1 mg/mL	GO 0.1
0.5 mg/mL	GO 0.5
1 mg/mL	GO 1
0.1 mg/mL	GO-ED 0.1
0.5 mg/mL	GO-ED 0.5
1 mg/mL	GO-ED 1
0.1 mg/mL	GO-ED-BA 0.1
0.5 mg/mL	GO-ED-BA 0.5
1 mg/mL	GO-ED-BA 1

in embryos and larvae were monitored daily with a stereomicroscope (SZX16 Olympus microscope + SC50 Olympus camera) [20]. At the end of the experiment, 10 larvae from each group were fixed in 10% neutral formalin for histopathology and immunohistochemical analysis.

### 2.5. Histopathological Examination

The taken larva samples were fixed in 4% paraformaldehyde solution for 48 h, embedded in paraffin blocks at the end of routine tissue follow-up procedures, and 4  $\mu\text{m}$  thick sections were stained with hematoxylin-eosin (HE) and examined with a light microscope (Olympus BX 51, JAPAN). Sections were evaluated as absent (-), mild (+), moderate (++) and severe (+++) according to their histopathological features.

### 2.6. Double Immunofluorescence Investigation

Tissue sections taken on the adhesive (poly-L-Lysin) slides for immunofluorescence examination were deparaffinized and dehydrated. Then, endogenous peroxidase was inactivated by keeping in 3%  $\text{H}_2\text{O}_2$  for 10 min. The tissues were boiled in 1% antigen retrieval (citrate buffer (pH+6.1) 100X) solution. Sections were incubated with protein block for 5 min to prevent nonspecific background staining in tissues. At the other step, primary antibodies (8 OHdG Cat No: sc-66036, Dilution Ratio: 1/100, US) were dripped onto the tissues and incubated in accordance with the instructions for use. Immunofluorescence

secondary antibody was used as a secondary marker (FITC Cat No: ab6785 Diluent Ratio: 1/1000) and kept in the dark for 45 min. Then, second primary antibodies (TNF- $\alpha$  Cat No: sc-52746, Dilution Ratio: 1/100, US) were dripped onto the tissues and incubated in accordance with the instructions for use. Immunofluorescence secondary antibody was used as a secondary marker (Texas Red Cat No: ab6719 Diluent Ratio: 1/1000 UK) and kept in the dark for 45 min. At the last stage, DAPI with mounting medium (Cat no: D1306 Dilution Rate: 1/200 UK) was dripped onto the sections and kept in the dark for 5 min, and the sections were closed with a coverslip. The stained sections were examined under a fluorescent microscope (Zeiss Axio Germany) and the data were evaluated in the Zeiss Zen Imaging Software.

## 2.7. Data analysis and statistics

Post-hoc analyses were conducted by using Tukey's multiple comparison test. We used the Turkey test because the samples' count in each group is equal and same, as well as reducing the probability of obtaining false positives. In this study, all values are presented as mean  $\pm$  standard error of mean, and differences were considered statistically significant at  $***p < 0.0001$ ,  $**p < 0.001$ ,  $*p < 0.01$ , and  $p < 0.05$ . Statistical analysis was performed using SPSS version 25.0 and GraphPad Prism 8.

For histopathological results; The data were evaluated with the SPSS 13.0 program and  $p < 0.05$  was considered significant. Duncan test was used for comparison among groups. The Kruskal-Wallis test was used to detect group interaction, and the Mann Whitney U test was used to determine the differences between groups.

For immunofluorescent staining findings; In order to determine the intensity of positive staining from the obtained images, 5 random areas were selected from each image and evaluated in the Zeiss Zen Imaging Software program. Data were statistically defined as mean and standard deviation (mean $\pm$ SD) for % area. Mann-Whitney U test was performed to compare positive immunoreactive cells and immunopositive stained areas with healthy controls. As a result of the test, an AP value of  $< 0.05$  was considered significant and the data were presented as mean  $\pm$  SD.

## 3. Results

### 3.1. Characterization of GO-ED-BA nanoparticles

Characterizations of new graphene oxide derivatives were performed with FT-IR, SEM, TEM and BET analysis. It was determined that the surface became smaller with the modification of the amine group and boric acid, respectively. In this study, all characterization results will be the first examples of graphene oxide-boramic acid nanostructure because we have reported graphene oxide-boramic acid nanostructure for the first time.

## 4. FT-IR Analysis

FT-IR spectra were obtained using KBr pellets ( $4000\text{--}400\text{ cm}^{-1}$ ) on Bio-Rad-Win-IR Spectrophotometer. GO-ED shows a vibration band at  $2095\text{ cm}^{-1}$ . The peak of GO-ED, ( $2095\text{ cm}^{-1}$ ) can be associated with the C-N functional group. GO-ED-BA shows vibration band at  $3308\text{ cm}^{-1}$ ,  $2133\text{ cm}^{-1}$ ,  $1684\text{ cm}^{-1}$ ,  $1399\text{ cm}^{-1}$ ,  $1315\text{ cm}^{-1}$ ,  $1159\text{ cm}^{-1}$ ,  $923\text{ cm}^{-1}$ ,  $775\text{ cm}^{-1}$ ,  $701\text{ cm}^{-1}$ . GO-ED-BA; Vibrations in the band range of  $3300\text{--}3500\text{ cm}^{-1}$  might be due to OH groups in boric acid, the vibration of  $2133\text{ cm}^{-1}$  is because of C-N functional group,  $1684\text{ cm}^{-1}$  with amide group,  $1399\text{ cm}^{-1}$  with N-H groups,  $1159\text{ cm}^{-1}$  and other vibration bands with  $923\text{ cm}^{-1}$ ,  $775\text{ cm}^{-1}$ , and  $701\text{ cm}^{-1}$  might be associated with N-B, and B-O functional groups [23,26,39,43,24] (Fig. 4).

## 5. SEM Analysis

Structure characterization of the samples was performed using a Zeiss Sigma 300 scanning electron microscope (SEM) with SE detector at

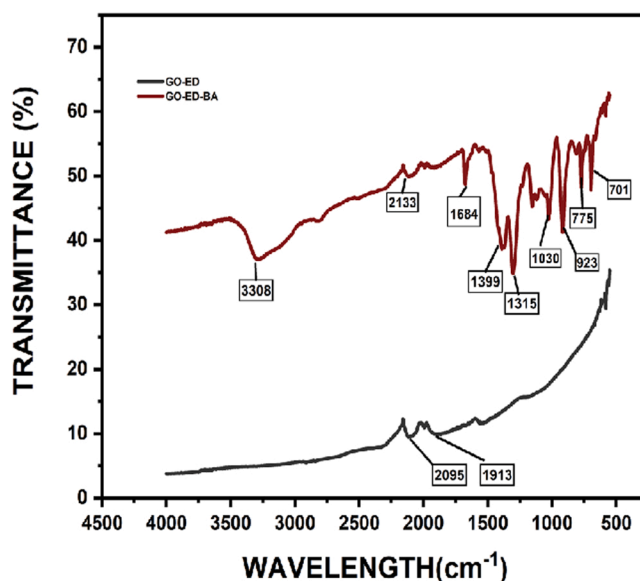


Fig. 4. FT-IR images of GO-ED and GO-ED-BA.

10 kV acceleration voltage. SEM images of GO-ED (a) and GO-ED-BA (b) are given in Fig. 5. SEM images revealed that after amination of GO, the surface was composed of randomly clustered layers forming a more porous and disordered network [22]. In addition, it was determined that the surface became rougher after amination and boric acid modification [39] (Fig. 5).

## 6. TEM Analysis

The dark areas represent oxygen-containing functional groups (such as carboxyl groups) on the GO surface and the stacked structure of several GO layers. The transparent areas indicate the thinned structure of the layer resulting from the exfoliation of the stacked GO layer. Stobinski et al., (2018) [31]. As shown in Fig. 6, the TEM image of GO-ED shows that the surface has rougher and more curved edges compared to GO. In addition, it was determined that the amine group modification did not cause any damage to the structure of the GO layer [38]. As seen in the TEM image, it was seen that the surface was more curved and more roughness occurs with boric acid modification compared to GO-ED [28]. As seen in Fig. 6, it was determined that the GO thickness ranged from the center of the basal plane to the edges ( $0.883\text{--}1.565\text{ nm}$ ), and the average single-layer GO layers were approximately  $1.044\text{ nm}$ . In addition, the mean values of GO-ED and GO-ED-BA were determined as  $0.43525\text{ nm}$  and  $0.47475\text{ nm}$ , respectively [30] [12] (Fig. 6). On the other hand, due to the fact that graphene oxide-boramic acid nanostructure was reported for the first time in this study, we could not compare our TEM results with the literature reports in detail.

## 7. BET Analysis

BET helped with surface analysis is a very useful measurement technique for the surface area and porosity of the prepared materials. The rate of surface area to volume of the prepared nanomaterial plays a very important role in definition some the properties of the materials [36]. Fig. 7 shows the  $\text{N}_2$  adsorption/desorption isotherms for the pristine GO, GO-ED, and GO-ED-BA samples at 77 K. Table 2 shows the distribution of surface area and pore volume for different samples such as GO, GO-ED and GO-ED-BA. Loading of the ED and BA groups on the surface area leads to a reduction in the specific surface area. Compared with the pristine GO sample, the GO-ED and GO-ED-BA modified treatments are thought to cause shrinkage or decreasing of the pure GO micropores [43].

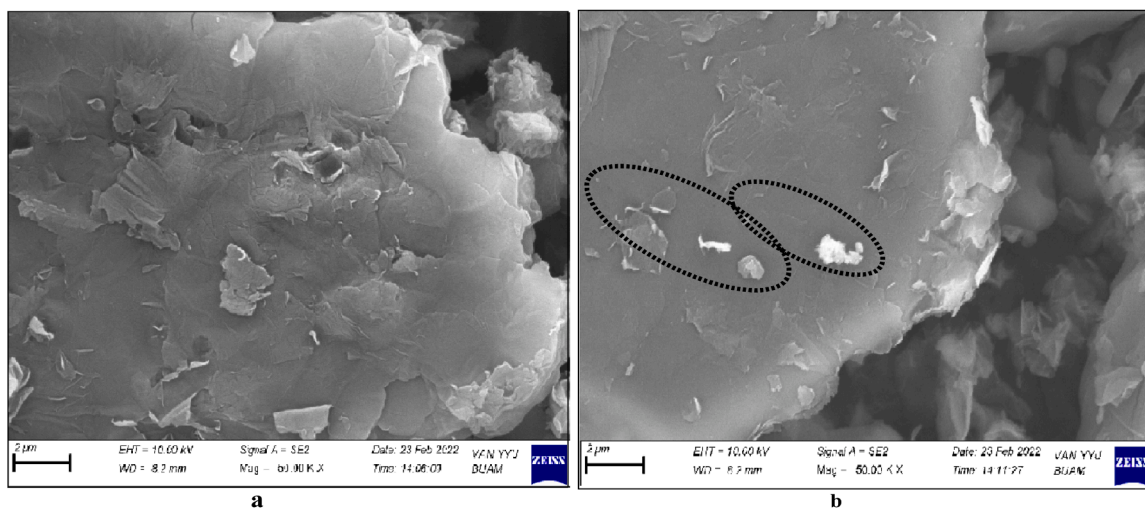


Fig. 5. SEM images of GO-ED and GO-ED-BA.

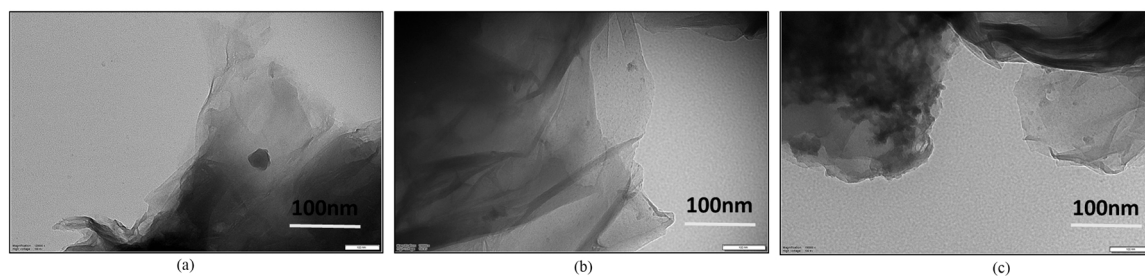


Fig. 6. TEM images of GO (a), GO-ED (b) and GO-ED-BA (c).

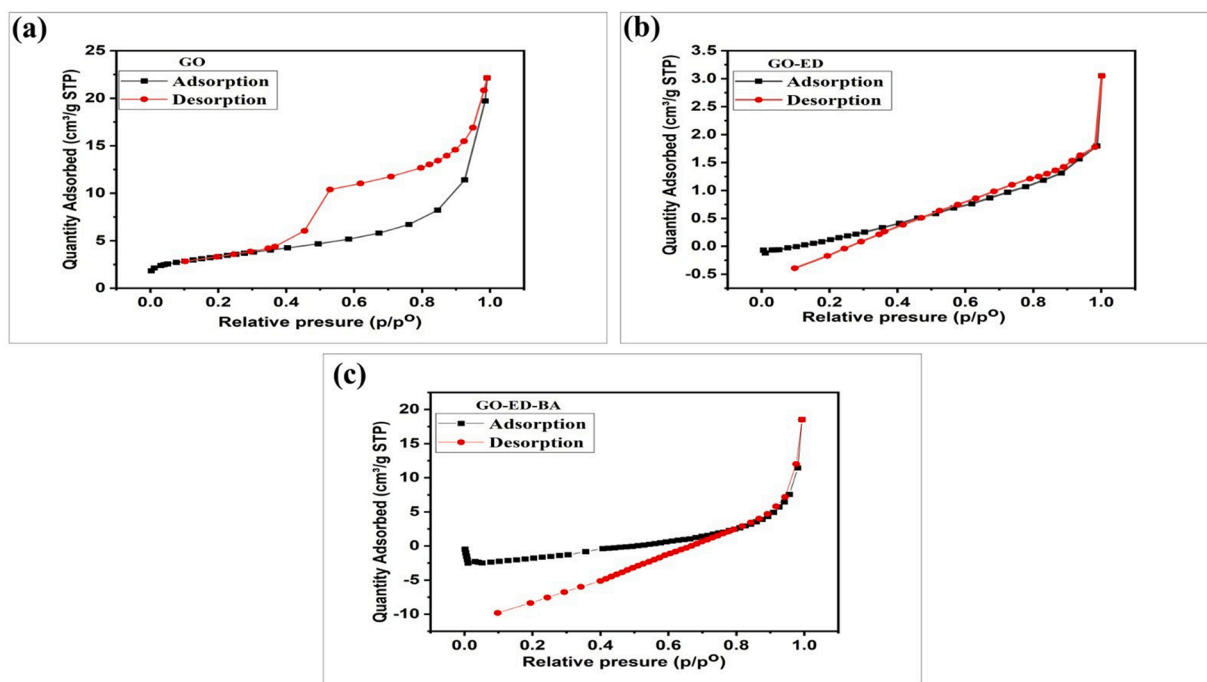


Fig. 7. BET graphs for GO, GO-ED and GO-ED-BA.

### 8. Nanotoxicity on Zebrafish embryos/larvae

When developmental toxicity to zebrafish embryos was assessed for

GO-ED-BA NP and its components GO and GO-ED, the survival rates determined between 4 and 96 h after fertilization are given in Fig. 8. In the comparison of the control and DMSO groups with the treatment

**Table 2**

Surface properties and chemical composition of pristine and modified GO samples on the BET device.

	GO (m <sup>2</sup> /g)	GO-ED (m <sup>2</sup> /g)	GO-ED-BA (m <sup>2</sup> /g)
SBET (m <sup>2</sup> /g)	7,4646	1,4671	0,4669
Pore Volume(cm <sup>3</sup> /g)	0,019153	0,002504	0,010833

groups, no difference was found in the 0.1 mg/mL GO-ED and GO-ED-BA groups at the  $p < 0.05$  level (Fig. 8). However, significant and/or very important changes were determined between the other application groups and the control - DMSO groups. While the highest survival rate (over >90%) was determined in the 0.1 and 0.5 mg/mL GO-ED-BA NP groups, this rate decreased to an average of 67% in the high concentration (1 mg/mL) groups.

Some morphological abnormalities (yolk sac edema, lordosis/kyphosis, pericardial edema, and tail malformation) were observed in embryos and larvae exposed to GO, GO-ED and GO-ED-BA NP for 96 h (Fig. 9). The highest total abnormality was detected in the GO 1 mg/mL group with 34%, and the difference was very significant ( $p < 0.0001$ ) when compared with the control and DMSO groups (Fig. 10). Similarly, it was found that there was a significant increase in the morphological changes of GO-ED-BA NP at all application doses compared to the control and DMSO groups (\*\*\*\* $p < 0.0001$ , \*\*\* $p < 0.001$ ) (Fig. 10).

In embryos treated with 1 mg/mL GO-ED-BA NP, there was a delay in larval hatching compared to control and other administration groups (Fig. 11). Larval emergence rates of GO-ED-BA NP were found to be 95% at 0.1 mg/mL at 96th hour, 93% at 0.5 mg/L and 68% at 1 mg/mL (Fig. 11). At low GO doses (0.1 mg/mL: 90%, 0.5 mg/mL: 88%) larvae hatching rates were lower than the same concentrations of BA-bound nanoparticles (GO-ED-BA NPs).

Interestingly, no teratogenicity was observed at the lowest concentrations of GO-ED-BA NPs (0.1 and 1 mg/mL) and showed a normal architecture very similar to the control embryo. These results clearly demonstrated the significantly lower toxicity of GO-ED-BA NP nanocomposite compared to GOs, which means that binding of boramic acid on graphene oxide surface might lead to some important impacts on modification when further biological applications might be desired.

## 9. Histopathological Findings

When the larval tissues of the control and DMSO groups were

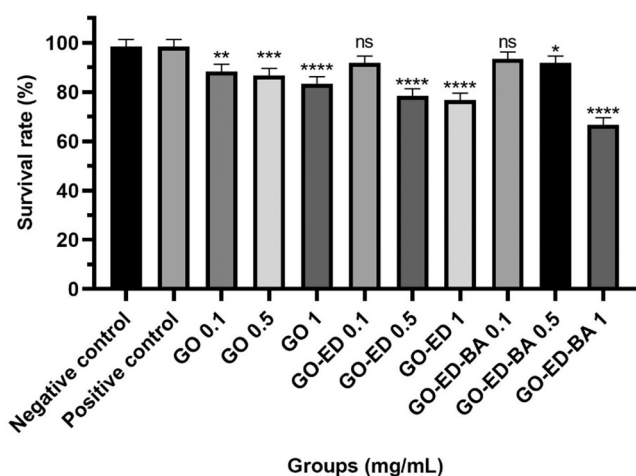


**Fig. 8.** Survival rates in zebrafish embryos and larvae exposed to different concentrations of GO, GO-ED, and GO-ED-BA NPs. Treatment groups were determined using one-way ANOVA with Tukey's post hoc test. ns: not significant, \*\*\*\* $p < 0.0001$ , \*\*\* $p < 0.001$ , \*\* $p < 0.01$ , \* $p < 0.05$ , and ns: not significant.

examined histopathologically, it was determined that they had a normal histological appearance (Fig. 12). On the other hand, in GO applications, the level of severity in histopathological findings increased from low concentration to high concentration groups. The findings are summarized for all application groups in Fig. 12.

0.1 mg/mL GO: When the larval tissues were examined histopathologically, moderate degeneration and very mild necrosis were observed in neurons (Fig. 12). 0.5 mg/mL GO: In the larval tissues' histopathological examination, severe degeneration and mild necrosis were detected in neurons (Fig. 12). 1 mg/mL GO: Severe degeneration and moderate necrosis were observed in the neurons of the larval tissues (Fig. 12). 0.1 mg/mL GO-ED: When the larval tissues were examined histopathologically, very mild degeneration was detected in the neurons (Fig. 12). 0.5 mg/mL GO-ED: Mild degeneration was observed in the neurons of the larval tissues (Fig. 12). 1 mg/mL GO-ED: Moderate degeneration and very mild necrosis were detected in neurons (Fig. 12). 0.1 mg/mL GO-ED-BA: Mild degeneration of neurons was seen (Fig. 12). 0.5 mg/mL GO-ED-BA: When the larval tissues were examined histopathologically, moderate degeneration and very mild necrosis were detected in neurons (Fig. 12). 1 mg/mL GO-ED-BA: Severe degeneration and mild necrosis were observed in neurons (Fig. 12). Histopathological findings are summarized in Table 3.

Histopathological findings show that modification of graphene oxide with ethylene diamine and boric acid influences the rate of degeneration and necrosis in neurons of the zebrafish. All concentrations of modified GO samples displayed lower toxicity on neurons than GO did, which means that further modification with similar functionality might give more nontoxic nanoparticles.

## 10. Immunofluorescent findings

When the immunofluorescence staining of the larval tissues was examined, 8 OHdG (8-hydroxy-2'-deoxyguanosine) and TNF- $\alpha$  (Tumor Necrosis Factor) expression were evaluated as negative (Fig. 12). Findings of other application groups were;

0.1 mg/mL GO: When the immunofluorescent staining of the larval tissues was examined, moderate cytoplasmic 8 OHdG expression in neurons and moderate TNF- $\alpha$  expression around vessels and tissue spaces were determined (Fig. 12). 0.5 mg/mL GO: Severe cytoplasmic 8 OHdG expression was observed in neurons, and severe TNF- $\alpha$  expression was observed around the vessels (Fig. 12). 1 mg/mL GO: Too severe cytoplasmic 8 OHdG expression in neurons, and very severe TNF- $\alpha$  expression in the interstitium around the vessels (Fig. 12). 0.1 mg/mL GO-ED: very mild expression of 8 OHdG was seen in neurons, and very mild expression of TNF- $\alpha$  was observed around the vessels and in the interstitium (Fig. 12). 0.5 mg/mL GO-ED: When the immunofluorescent staining of the larval tissues was examined, mild cytoplasmic 8 OHdG expression in neurons and mild TNF- $\alpha$  expression around vessels and interstitium were determined (Fig. 12). 1 mg/mL GO-ED: moderate intracytoplasmic 8 OHdG expression in neurons, moderate TNF- $\alpha$  expression around vessels and interstitium were detected (Fig. 12). 0.1 mg/mL GO-ED-BA: Mild expression of 8 OHdG was observed in neurons, and mild expression of TNF- $\alpha$  was observed around vessels (Fig. 12). 0.5 mg/mL GO-ED-BA: moderate cytoplasmic 8 OHdG expression in neurons and moderate TNF- $\alpha$  expression around vessels were determined (Fig. 12). 1 mg/mL GO-ED-BA: When the immunofluorescent staining of the larval tissues was examined, intense cytoplasmic 8 OHdG expression in neurons and severe TNF- $\alpha$  expression around the vessels were determined (Fig. 12). Immunofluorescent findings are summarized in Table 4. Statistical analysis results of 8 OHdG and TNF- $\alpha$  expressions in larval tissues.

Table 4 indicated that two important markers, for biological evaluation were expressed with. As can be seen in Table 4, it was determined that the levels of two important markers, 8-OHdG and TNF- $\alpha$ , were the highest after interactions with pure GO. This was similar to other toxicity experiments conducted in this study. In the immunofluorescent

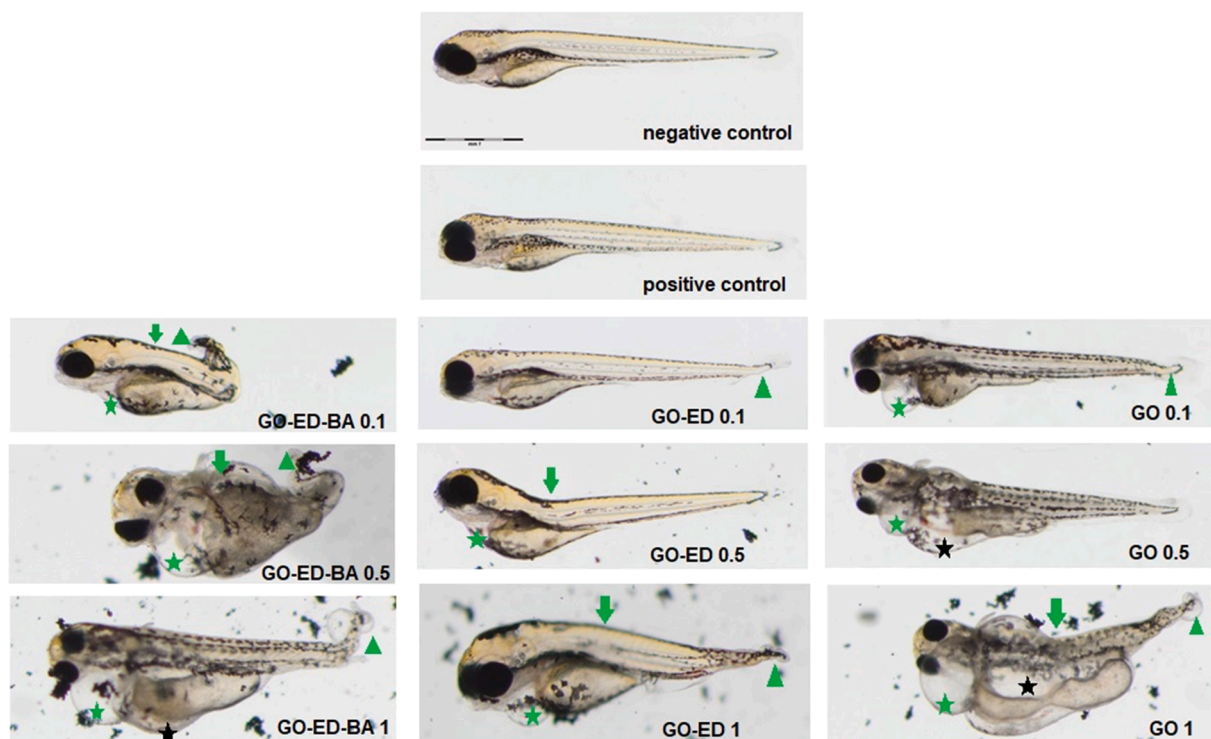


Fig. 9. Microscopic images of the abnormalities observed in zebrafish embryos/larvae at 96 hpf. Black star: Yolk sac edema, green arrow: Lordosis/kyphosis, green star: Pericardial edema, green arrowhead: Tail malformation. Scale bar: 1mm (2.5X).

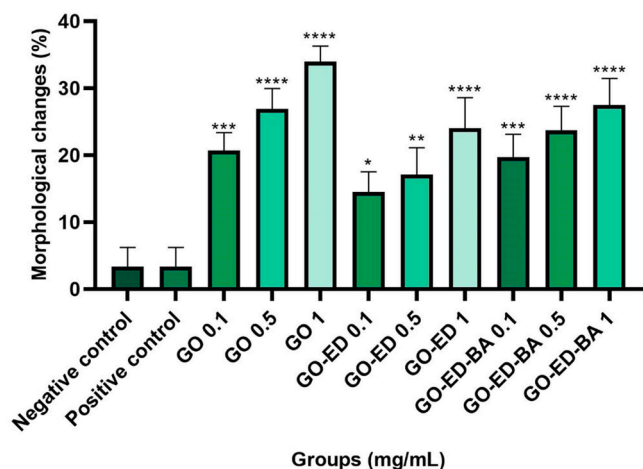


Fig. 10. Morphological changes in zebrafish embryos/larvae exposed to different concentrations of GO, GO-ED, and GO-ED-BA NPs. Data are expressed as means  $\pm$  S.D. from three independent experiments ( $n=20$ ) one-way ANOVA with Tukey's post hoc test. ns: not significant, \*\*\*\* $p < 0.0001$ , \*\*\* $p < 0.001$ , \*\* $p < 0.01$ , and \* $p < 0.05$ .

findings, it was observed that DNA damage was reduced by the modification of the GO surface with amine and boric acid, which could be a good start for a more environmentally friendly alternative nanoparticle production.

According to the histopathological and immunofluorescent results, it was observed that the brain tissues were damaged only in the GO treated groups, and the expression levels of TNF- $\alpha$ , which is a proapoptotic and inflammatory marker, increased its severity depending on the dose. At the same time, a dose-dependent increase was observed in 8 OHdG expression levels, a marker of DNA damage. A statistically significant difference was found in the expression levels of TNF- $\alpha$  and 8 OHdG in

the alone amine groups (GO-ED) with GO application compared to the GO groups, especially at low doses. Although there was a difference in the expression levels of TNF- $\alpha$  and 8 OHdG in the groups (GO-ED-BA) treated with boric acid together with the amine, these differences were not statistically significant.

## 11. Discussion

In the study where we characterized the superstructure of GO with TEM and SEM images, it was determined that there are irregular folds observed in the GO nanolayers, reflecting the flexibility of the GO nanolayers. These results confirmed that the used nanomaterial was typical GO and in agreement with previous studies [37]. Consistent with previous work, impairment in ROS generation and genetic expression through graphene family nanoparticle (GFN) internalization and physical interaction, including adsorption on the cell surface, can be attributed to differential surface oxidation or different toxicological mechanisms. Besides these aspects, there may be other factors (other than size and oxidation state) that influence the toxic behavior of G and GO in cells [16].

While graphene and its derivatives are of great interest for their potential applications in biomedical fields, the information is too little about their toxicity and biocompatibility in aquatic organisms [13]. Zebrafish embryo is a widely used and successful animal model to evaluate the toxicity of nanomaterials and unravel the mechanism behind the toxicity [8]. In embryos, hatchability is a motility issue. In our findings, the low larval emergence rate in low-dose GO applications as well as high concentration of GO-ED-BA NP can be explained by the fact that GO adheres to the embryo, restricting movement and creating a hypoxic environment [12]. In a study conducted in line with our findings, it was reported that GO particles adhere to the zebrafish embryo chorion with the help of hydroxyl interactions and can pass into the pore channels by passive diffusion [11]. The ability of nanoparticles to penetrate the chorion is an important factor in experimental design influencing their toxicology profile [25]. Bangeppagari et al. [8]

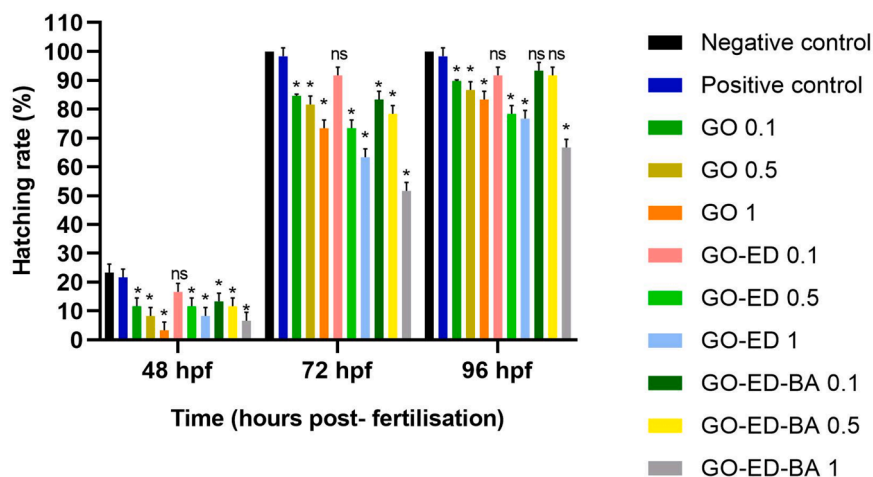


Fig. 11. Hatching rate of zebrafish embryos exposed to different concentrations of GO, GO-ED, and GO-ED-BA NP. Data are expressed as means  $\pm$  S.D. from three independent experiments ( $n=20$ ) one-way ANOVA with Tukey's post hoc test. ns: not significant, and  $*p < 0.05$ .

reported that graphene oxide causes significant embryonic mortality, increased heart rate, delayed hatching, cardiotoxicity, cardiovascular defects, delayed cardiac cycle, increased apoptosis, and decreased hemoglobinization in zebrafish. Contrary to this study, although GO-ED-BA NP's small size, it is thought that synthesis by-products, especially BA, are effective in not being as toxic as GO. In different zebrafish researches, it had been reported that BA and its derivatives have protective effects [3,2,4]. The previous studies had reported that boron and its derivatives are effective not only in the activity of many enzymes, but also in hormone and lipid metabolisms [32,33] and can be used safely in aquatic environments [5].

In our study, toxic effects increased in direct proportion to nanocomposite concentrations. At 1.0 mg/mL of GO-ED-BA NP, higher toxicity was found to be associated with reduced growth with some morphological defects, whereas at lower doses (0.1 and 0.5 mg/mL) these deformations were not significant. The findings of Krishnaraj et al. [21] confirm our data.

Our results showed that GO particles cause different degrees of deformity, mainly including pericardial edema, yolk sac edema, tail curvature and spinal curvature in zebrafish. These results were consistent with Chen et al. [12], Bangeppagari et al. [8] and Chen et al. [11] reports. Although it had not yet been clarified whether leaching of GO and other nanomaterials through a water system impairs the function of the system, only a few studies had included advanced omic techniques to get detailed information on GO nanotoxicity. In these studies, GO enters the zebrafish body through water and had been reported to affect embryonic development by increasing ROS production, damaging mitochondria, and inducing genotoxicity and metabolic dysfunction [8].

DNA damage is an important issue as it can lead to serious problems such as mutations, cell death and apoptosis. Therefore, precise and easy detection of damage is an obligation [18]. In the light of histopathological and immunohistochemical data, the increases in DNA damage and TNF- $\alpha$  levels, especially in GO groups, can be explained by the penetration of GO into the chorion and the production of excessive reactive oxygen species in the organs, oxidative stress, DNA damage and increased apoptosis [11]. Zhang et al. [42] reported that the accumulation of ROS can damage and alter DNA structure in organisms. 8-OHdG, the main product of DNA oxidation, has stable chemical properties as an oxidative adduct produced by DNA molecules attacking ROS. The results showed that the 8-OHdG content increased significantly in parallel with the increase in concentration at all GO concentrations. This increase is thought to be a response to oxidative damage. Again, the high level of 8-OHdG determined at all GO doses and the high dose of the synthesis product GO-ED-BA NP is interpreted as that the compound in question induces DNA damage with hydroxyl radicals

(GO) [18]. It had been reported that GFN negatively affects the expression patterns of genes related to cell growth, differentiation, DNA damage and metabolism [16].

Neurotoxicity is an etiological phenomenon of alteration in the structure and function of the central nervous systems by an agent (biological, chemical or physical) [7]. Although the neuroendocrine system and the immune system act independently of each other a widespread communication network is thought to be under the control of a harmonious neuroendocrine-immune interaction [5,34].

GO-induced neurotoxicity was attenuated at low concentrations (0.1 and 0.5 mg/mL) co-administered with BA, as confirmed by elevated brain neurotransmitters with marked changes in TNF- $\alpha$  levels. This situation can be explained by the fact that GO leads to the stimulation of inflammatory cells by releasing several cytokines and increasing the expression levels of inflammation-related genes. Since there are no studies of GO-ED-BA NP in aquatic organisms, there are limitations to comparisons that can be made in the current literature. TNF- $\alpha$  had been reported to play an important role in emotional regulation in organisms. It had been stated that increased anxiety behaviors are effective in the overexpression of TNF- $\alpha$  in the brain [15]. Our results, where we noticed that GO exerted higher oxidative and genotoxic stress on cells than BA, can be attributed to the higher surface activity of GO materials compared to complementary by-products (ED-BA). Consistent with these recommendations, we can say that GO-induced stress increases TNF- $\alpha$  levels.

## 12. Conclusion

Our studies showed that GO causes malformation and death, neurological impairment in zebrafish embryos, and that GO can trigger oxidative stress, immune cells, and inflammatory responses. Graphene oxide-based GO-ED-BA NP was not as cytotoxic as GO at low concentrations, but induced proinflammatory and oxidative stress responses. The increased cytotoxicity at the highest concentration was potentially caused by its reduced diameter (observed in this case only). Again, the biological activity and physicochemical changes of the materials also showed a direct effect due to malformations and alterations in neurotoxicity. When our results are evaluated collectively, it is important to be careful in the integration of modified products in GO-based nanoparticles, and to determine the toxicological profile and exposure time of its components, especially for low concentration applications, for a good risk management.

Hazard and exposure factors need to be evaluated in risk assessment in aquatic ecosystems. In this study, we describe the toxicological profiles of ED and BA integration byproducts for GO-based nanoparticles. It

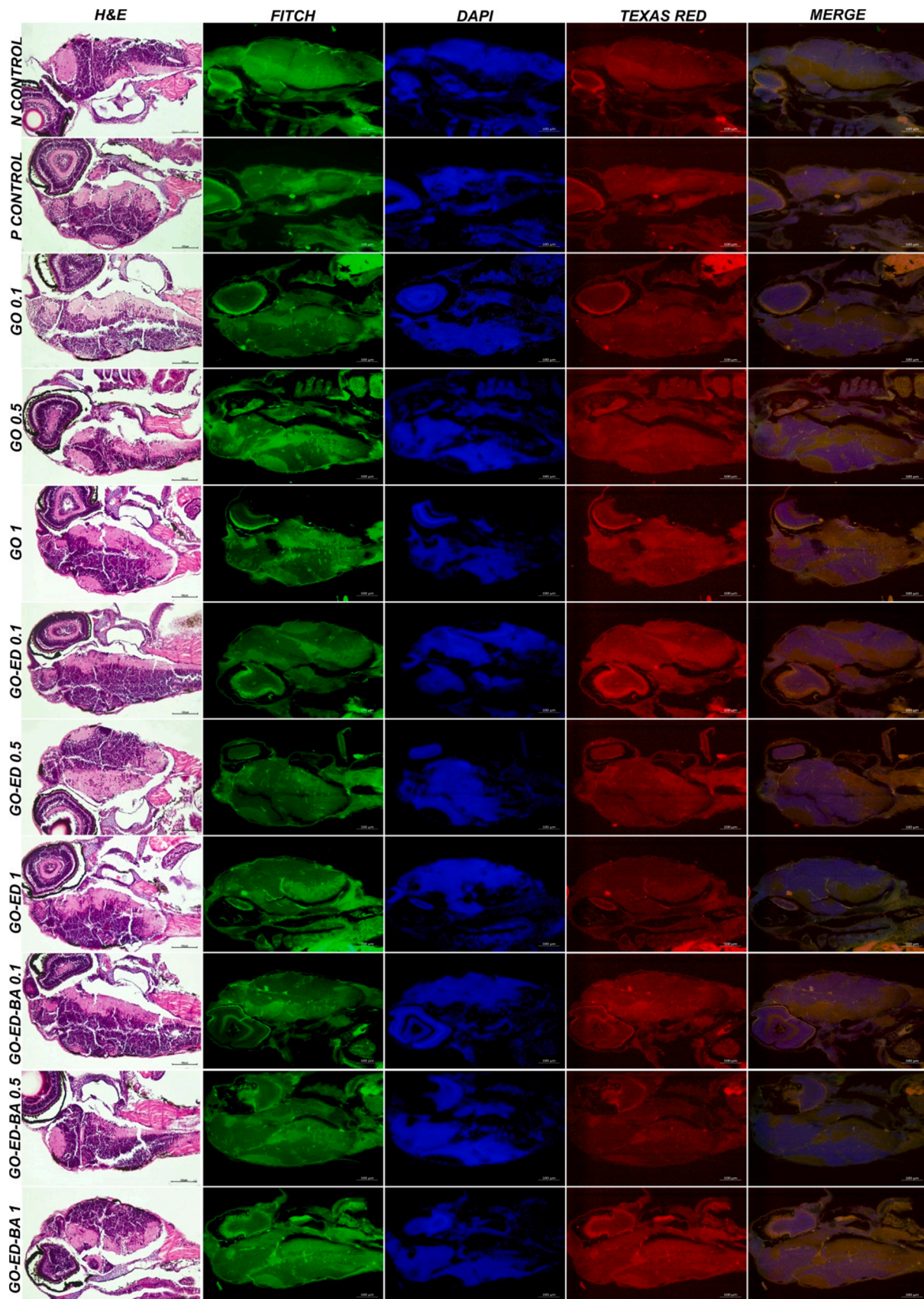


Fig. 12. Larval samples, Histopathological findings, H&E, 8 OHdG expressions (FITC), TNF- $\alpha$  expression (Texas Red), IF, Bar: 100 $\mu$ m.

Table 3

Scoring of histopathological findings observed in larval tissues.

Treatment group	Degeneration in Neurons	Necrosis in Neurons
Control	–	–
DMSO	–	–
GO 0.1 mg/mL	+++	+
GO 0.5 mg/mL	++++	++
GO 1 mg/mL	+++++	+++
GO-ED 0.1 mg/mL	+	–
GO-ED 0.5 mg/mL	++	–
GO-ED 1 mg/mL	+++	+
GO-ED-BA 0.1 mg/mL	++	–
GO-ED-BA 0.5 mg/mL	+++	+
GO-ED-BA 1 mg/mL	++++	++

Table 4

Expression levels of 8-OHdG and TNF- $\alpha$  in zebrafish tissues after treatments with different doses.

Treatment group	8-OHdG	TNF- $\alpha$
Control	21.18 $\pm$ 6.12 <sup>a</sup>	20.84 $\pm$ 6.73 <sup>a</sup>
DMSO	23.86 $\pm$ 4.48 <sup>a</sup>	22.16 $\pm$ 5.18 <sup>a</sup>
GO 0.1 mg/mL	60.26 $\pm$ 8.93 <sup>bf</sup>	57.63 $\pm$ 8.75 <sup>bf</sup>
GO 0.5 mg/mL	76.74 $\pm$ 9.16 <sup>bcd</sup>	73.85 $\pm$ 9.18 <sup>bcd</sup>
GO 1 mg/mL	94.18 $\pm$ 9.94 <sup>cd</sup>	90.18 $\pm$ 9.97 <sup>cd</sup>
GO-ED 0.1 mg/mL	33.92 $\pm$ 6.85 <sup>ae</sup>	30.74 $\pm$ 6.94 <sup>ae</sup>
GO-ED 0.5 mg/mL	44.18 $\pm$ 8.59 <sup>bef</sup>	42.76 $\pm$ 8.14 <sup>bef</sup>
GO-ED 1 mg/mL	58.38 $\pm$ 9.12 <sup>bdf</sup>	57.24 $\pm$ 9.18 <sup>bdf</sup>
GO-ED-BA 0.1 mg/mL	45.15 $\pm$ 8.84 <sup>bef</sup>	42.19 $\pm$ 9.27 <sup>bef</sup>
GO-ED-BA 0.5 mg/mL	59.92 $\pm$ 8.19 <sup>bef</sup>	56.73 $\pm$ 8.74 <sup>bef</sup>
GO-ED-BA 1 mg/mL	77.61 $\pm$ 9.92 <sup>bcd</sup>	73.18 $\pm$ 9.16 <sup>bcd</sup>

a,b,c,d,e,f: Different letters in the same column were considered statistically different ( $p < 0.05$ )

should be interesting to complement this study with an assessment of exposure of zebrafish embryo/larvae. Because, as a known situation, such synthesis products can be diffused in soil or water parts, they can be exposed indirectly (through food, water) to humans as well as ecosystems. Therefore, this research's findings are attractive for the ecotoxicology field.

#### CRedit authorship contribution statement

**Mine Köktürk:** The owner of research idea and Formal analysis. **Serkan Yıldırım:** Resources, Formal analysis. **Aybek YİĞİT:** Green synthesis. **Gunes Ozhan:** Writing – review & editing. **Muhammed Atamanalp:** Resources, Formal analysis. **Mehmet Hakkı Alma:** Resources, Formal analysis. **Ismail Bolat:** Resources, Formal analysis. **Nurettin Menges:** Green synthesis. **Muhammed Atamanalp:** Conceptualization, Visualization, Writing – review & editing. **Nurettin Menges:** Conceptualization, Visualization, Writing – review & editing. **Gonca Alak:** Formal analysis, Visualization, Writing – original draft, Writing – review & editing. All the authors read and approved the final version.

#### Declaration of Competing Interest

The authors declare that they have no known competing financial interests or personal relationships that could have appeared to influence the work reported in this paper.

#### Data Availability

Data will be made available on request.

#### References

- [1] S.F. Adil, M. Ashraf, M. Khan, M.E. Assal, M.R. Shaik, M. Kuniyil, M.N. Tahir, Advances in graphene/inorganic nanoparticle composites for catalytic applications, *Chem. Rec.* (2022), e202100274.
- [2] G. Alak, A.Ç. Yeltekin, A. Uçar, V. Parlak, H. Türkez, M. Atamanalp, Borax alleviates copper-induced renal injury via inhibiting the DNA damage and apoptosis in rainbow trout, *Biological trace element research* 191 (2) (2019) 495–501.
- [3] G. Alak, A. Ucar, A.Ç. Yeltekin, S. Çomaklı, V. Parlak, I.H. Taş, H. Türkez, Neuroprotective effects of dietary borax in the brain tissue of rainbow trout (*Oncorhynchus mykiss*) exposed to copper-induced toxicity, *Fish physiology and biochemistry* 44 (5) (2018) 1409–1420.
- [4] G. Alak, F.B. Özgeriş, A.Ç. Yeltekin, V. Parlak, A. Ucar, O. Çağlar, M. Atamanalp, Hematological and hepatic effects of ulexite in zebrafish, *Environmental Toxicology and Pharmacology* 80 (2020), 103496.
- [5] G. Alak, A. Ucar, V. Parlak, A.Ç. Yeltekin, F.B. Özgeriş, M. Atamanalp, H. Türkez, Antioxidant potential of Ulexite in Zebrafish brain: assessment of oxidative DNA damage, apoptosis, and response of antioxidant defense system, *Biological Trace Element Research* 199 (3) (2021) 1092–1099.
- [6] M. Arakha, S. Pal, D. Samantarrai, T.K. Panigrahi, B.C. Mallick, K. Pramanik, S. Jha, Antimicrobial activity of iron oxide nanoparticle upon modulation of nanoparticle-bacteria interface, *Sci. Rep.* 5 (1) (2015) 1–12.
- [7] I. Ashif, A. Musheer, A. Shah Nawaz, C.R. Sahoo, I.M. Kashif, S.E. Haque, Environmental neurotoxic pollutants, *Environ. Sci. Pollut. Res. Int.* 27 (33) (2020) 41175–41198.
- [8] M. Bangeppagari, S.H. Park, R.R. Kundapur, S.J. Lee, Graphene oxide induces cardiovascular defects in developing zebrafish (*Danio rerio*) embryo model: In-vivo toxicity assessment, *Sci. Total Environ.* 673 (2019) 810–820.
- [9] Z. Bian, A. Liu, Y. Li, G. Fang, Q. Yao, G. Zhang, Z. Wu, Boronic acid sensors with double recognition sites: a review, *Analyst* 145 (2020) 719–744.
- [10] M. Celebi, K. Karakas, I.E. Ertas, M. Kaya, M. Zahmakiran, Palladium nanoparticles decorated graphene oxide: active and reusable nanocatalyst for the catalytic reduction of hexavalent chromium (VI), *ChemistrySelect* 2 (27) (2017) 8312–8319.
- [11] Y. Chen, X. Hu, J. Sun, Q. Zhou, Specific nanotoxicity of graphene oxide during zebrafish embryogenesis, *Nanotoxicology* 10 (1) (2016) 42–52.
- [12] Y. Chen, J. Li, P. Yuan, Z. Wu, Z. Wang, W. Wu, Graphene oxide promoted chromium uptake by zebrafish embryos with multiple effects: Adsorption, bioenergetic flux and metabolism, *Science of The Total Environment* 802 (2022), 149914.
- [13] T.P. Dasari Shareena, D. McShan, A.K. Dasmahapatra, P.B. Tchounwou, A review on graphene-based nanomaterials in biomedical applications and risks in environment and health, *Nano-Micro Lett.* 10 (3) (2018) 1–34.
- [14] W. Gao, Y. Chen, Y. Zhang, Q. Zhang, L. Zhang, Nanoparticle-based local antimicrobial drug delivery, *Adv. Drug Deliv. Rev.* 127 (2018) 46–57.
- [15] Alaa M. Hammad, et al., Ceftriaxone reduces waterpipe tobacco smoke withdrawal-induced anxiety in rats via modulating the expression of TNF- $\alpha$ /NFkB, Nrf2, and GLT-1, *Neuroscience* 463 (2021) 128–142.
- [16] P.P. Jia, T. Sun, M. Junaid, L. Yang, Y.B. Ma, Z.S. Cui, D.S. Pei, Nanotoxicity of different sizes of graphene (G) and graphene oxide (GO) in vitro and in vivo, *Environ. Pollut.* 247 (2019) 595–606.
- [17] M. Kaushik, R. Niranjana, R. Thangam, B. Madhan, V. Pandiyarasan, C. Ramachandran, G.D. Venkatasubbu, Investigations on the antimicrobial activity and wound healing potential of ZnO nanoparticles, *Appl. Surf. Sci.* 479 (2019) 1169–1177.
- [18] H.K. Kaya, N. Haghmoradi, B.Y. Kaplan, F. Kuralay, Platinum nanoparticles loaded carbon black: reduced graphene oxide hybrid platforms for label-free electrochemical DNA and oxidative DNA damage sensing, *J. Electroanal. Chem.* 910 (2022), 116180.
- [19] M. Kokturk, S. Yıldırım, M.S. Nas, G. Ozhan, M. Atamanalp, I. Bolat, G. Alak, Investigation of the oxidative stress response of a green synthesis nanoparticle (RP-Ag/ACNPs) in zebrafish, *Biological Trace Element Research* 200 (6) (2022) 2897–2907.
- [20] M. Kokturk, S. Yıldırım, M.H. Calimli, M.S. Nas, F. Ibaokurgil, G. Ozhan, G. Alak, Perspective on green synthesis of RP-Pd/AC NPs: characterization, embryonic and neuronal toxicity assessment, *Int. J. Environ. Sci. Technol.* (2022) 1–12.
- [21] C. Krishnaraj, V.K. Kaliannagounder, R. Rajan, T. Ramesh, C.S. Kim, C.H. Park, S. I. Yun, Silver nanoparticles decorated reduced graphene oxide: eco-friendly synthesis, characterization, biological activities and embryo toxicity studies, *Environ. Res.* 210 (2022), 112864.
- [22] L. Lai, L. Chen, D. Zhan, L. Sun, J. Liu, S.H. Lim, J. Lin, One-step synthesis of NH<sub>2</sub>-graphene from in situ graphene-oxide reduction and its improved electrochemical properties, *Carbon* 49 (10) (2011) 3250–3257.
- [23] H.D. Liu, Z.Y. Liu, M.B. Yang, Q. He, Superhydrophobic polyurethane foam modified by graphene oxide, *J. Appl. Polym. Sci.* 130 (5) (2013) 3530–3536.
- [24] X. Liu, C.M. Renard, S. Bureau, C. Le Bourvellec, Revisiting the contribution of ATR-FTIR spectroscopy to characterize plant cell wall polysaccharides, *Carbohydrate Polymers* 262 (2021), 117935.
- [25] A.M. de Medeiros, L.U. Khan, G.H. da Silva, C.A. Ospina, O.L. Alves, V.L. de Castro, D.S.T. Martinez, Graphene oxide-silver nanoparticle hybrid material: an integrated nanosafety study in zebrafish embryos, *Ecotoxicol. Environ. Saf.* 209 (2021), 111776.
- [26] S.M. Mousavi, S.A. Hashemi, M. Arjmand, A.M. Amani, F. Sharif, S. Jahandideh, Octadecyl amine functionalized Graphene oxide towards hydrophobic chemical resistant epoxy Nanocomposites, *ChemistrySelect* 3 (25) (2018) 7200–7207.

- [27] P. Pal, S. Bhattacharjee, M.P. Das, Y.-B. Shim, B. Neppolian, B.J. Cho, P. Veluswamy, J. Das, Design of electrochemically reduced graphene oxide/titanium disulfide nanocomposite sensor for selective determination of ascorbic acid, *ACS Appl. Nano Mater.* 4 (2021) 10077–10089.
- [28] M. Singh, S. Kaushal, P. Singh, J. Sharma, Boron doped graphene oxide with enhanced photocatalytic activity for organic pollutants, *J. Photochem. Photobiol. A: Chem.* 364 (2018) 130–139.
- [29] V. Srimaneepong, H.E. Skallevoid, Z. Khurshid, M.S. Zafar, D. Rokaya, J. Sapkota, Graphene for antimicrobial and coating application, *Int. J. Mol. Sci.* 23 (1) (2022) 499.
- [30] S. Stankovich, R.D. Piner, S.T. Nguyen, R.S. Ruoff, Synthesis and exfoliation of isocyanate-treated graphene oxide nanoplatelets, *Carbon* 44 (15) (2006) 3342–3347.
- [31] L. Stobinski, B. Lesiak, A. Malolepszy, M. Mazurkiewicz, B. Mierzwa, J. Zemek, I. Bieloshapka, Graphene oxide and reduced graphene oxide studied by the XRD, TEM and electron spectroscopy methods, *J. Electron Spectrosc. Relat. Phenom.* 195 (2014) 145–154.
- [32] H. Turkez, M.E. Arslan, A. Tatar, A. Mardinoglu, Promising potential of boron compounds against Glioblastoma: In Vitro antioxidant, anti-inflammatory and anticancer studies, *Neurochemistry International* 149 (2021), 105137.
- [33] H. Turkez, F. Geyikoglu, A. Tatar, M.S. Keles, İ. Kaplan, The effects of some boron compounds against heavy metal toxicity in human blood, *Experimental and Toxicologic Pathology* 64 (1-2) (2012) 93–101.
- [34] A. Ucar, V. Parlak, F.B. Ozgeris, A.C. Yeltekin, M.E. Arslan, G. Alak, M. Atamanalp, Magnetic nanoparticles-induced neurotoxicity and oxidative stress in brain of rainbow trout: Mitigation by ulexite through modulation of antioxidant, anti-inflammatory, and antiapoptotic activities, *Science of The Total Environment* 838 (2022), 155718.
- [35] H.B. Westerfield (Ed.), *Inside CIA's private world: declassified articles from the agency's internal journal, 1955-1992*, Yale University Press, 1995.
- [36] T. Xia, M. Kovoichich, M. Liang, L. Madler, B. Gilbert, H. Shi, A.E. Nel, Comparison of the mechanism of toxicity of zinc oxide and cerium oxide nanoparticles based on dissolution and oxidative stress properties, *ACS nano* 2 (10) (2008) 2121–2134.
- [37] G. Xiong, Y. Deng, X. Liao, J.E. Zhang, B. Cheng, Z. Cao, H. Lu, Graphene oxide nanoparticles induce hepatic dysfunction through the regulation of innate immune signaling in zebrafish (*Danio rerio*), *Nanotoxicology* 14 (5) (2020) 667–682.
- [38] A. Yang, J. Li, C. Zhang, W. Zhang, N. Ma, One-step amine modification of graphene oxide to get a green trifunctional metal-free catalyst, *Appl. Surf. Sci.* 346 (2015) 443–450.
- [39] A. Yigit, P.T. Pınar, Y. Akinay, M.H. Alma, N. Menges, Nanotube-boramic acid derivative for dopamine sensing, *ChemistrySelect* 6 (24) (2021) 6302–6313.
- [40] B. Yuan, Y. Wang, G. Chen, F. Yang, H. Zhang, C. Cao, B. Zuo, Nacre-like graphene oxide paper bonded with boric acid for fire early-warning sensor, *J. Hazard. Mater.* 403 (2021), 123645.
- [41] W. Zhai, X. Sun, T.D. James, J.S. Fossey, Boronic acid-based carbohydrate sensing, *Chem. Asian J.* 10 (2015) 1836–1848.
- [42] X. Zhang, Q. Liu, X. Shi, A.M. Asiri, Y. Luo, X. Sun, T. Li, TiO<sub>2</sub> nanoparticles–reduced graphene oxide hybrid: an efficient and durable electrocatalyst toward artificial N<sub>2</sub> fixation to NH<sub>3</sub> under ambient conditions, *Journal of Materials Chemistry A* 6 (36) (2018) 17303–17306.
- [43] Y. Zhang, Y. Chi, C. Zhao, Y. Liu, Y. Zhao, L. Jiang, Y. Song, CO<sub>2</sub> adsorption behavior of graphite oxide modified with Tetraethylenepentamine, *J. Chem. Eng. Data* 63 (1) (2018) 202–207.